

# Non-destructive Analysis for Metal/Glass Interface Using Synchrotron Radiation

Junji IHARA\* and Koji YAMAGUCHI

We have developed a new technique to analyze an interface between metal and glass nondestructively at Hermetic seal in electronic components. In the specimen fabrication, we employed a precise thinning technique instead of the conventional exfoliating, so that the interface would maintain its original state. In the diffraction measurements, we combined a highly brilliant x-ray from synchrotron radiation and 2-dimensional detector. By optimizing the specimen configuration, x-ray beam shape and its alignment, we succeeded in detecting diffraction peaks from a very small quantity of oxides that existed in the 1  $\mu\text{m}$  thick metal/glass interface.

Keywords: hermetic seal, synchrotron radiation, SPring-8, x-ray diffraction, metal/glass interface

## 1. Introduction

In the terminals of electronic components, the metal lead wires are often sealed with glasses in order to improve their environmental durability. The mechanical strength and airtightness at the metal/glass interface are of particularly great importance to create highly reliable products. The characteristics of the interface layer, where the metal and glass contact with each other, are considered to be affected by such factors as flatness, composition, and structure.

The scanning electron microscopy (SEM) and x-ray diffraction (XRD) analyses are conventionally employed for the characterization of the interface layer. In these analyses, the interface needs to be peeled off on one side. However, it is very difficult to perform the peeling process precisely. Besides, the exposure may change the state of the interface layer by oxidation.

**Figure 1** shows an SEM image of the wire/glass interface. The specimen is an airtight terminal of a cold cathode fluorescence lamp (CCFL), in which the Kovar or iron-based metal alloy wire is sealed with silicate glass. The SEM specimen was fabricated by using the cross-section polishing technique. We can clearly see the interface oxide layer, whose thickness is less than 1  $\mu\text{m}$ .

We fabricated another specimen by peeling off the glass side. From the SEM analysis, the exposed surface was found to have a fine granular texture, as shown in **Fig. 2 (a)**.

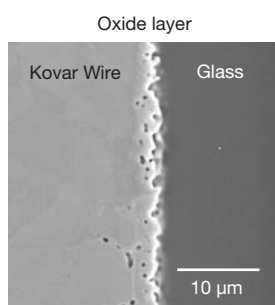


**Fig. 1.** SEM image of the interface between Kovar wire and glass

Though the residual Kovar side had been expected to show only the signals of Fe, Co, Ni, and their oxides, the energy dispersive x-ray spectrometry (EDX) analysis clarified that the exposed surface also contained Si, which should be derived from the silicate glass (**Fig. 2 (b)**). These results demonstrate that the specimen fabrication by peeling the surface cannot necessarily expose the aimed interface.

We also performed the XRD analyses, expecting to detect the Fe oxide on the exposed surface. In the measurement, we placed several specimens side by side to increase the intensity of diffraction signals. However, we detected no diffraction peak of Fe oxide on the Kovar side, as shown in **Fig. 3**. The same results were obtained from XRD analyses for the silicate glass side.

These results can be attributed to the following two reasons: one is that the remaining silicate glass made the exposed Kovar area very small, and the other is that the quantity of Fe oxide at the interface layer was too small to be detected by the x-ray source in the conventional XRD equipment.

To solve these problems, we have developed a new technique for fabricating a specimen without the peeling process. Considering the small quantity of the interface layer, a highly brilliant x-ray source was required for the XRD measurements.

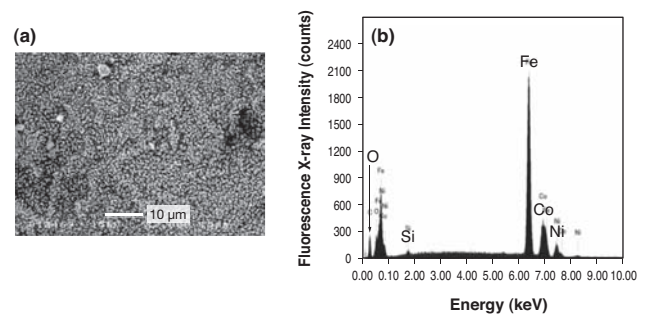


**Fig. 2.** Results of SEM and EDX analyses for peeled surface at Kovar wire and glass interface. (a) SEM image (b) Fluorescence x-ray spectrum

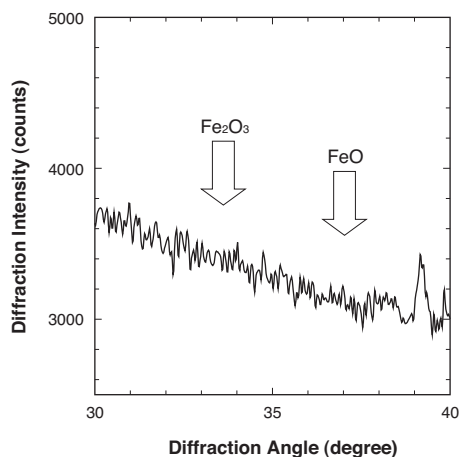


Fig. 3. X-ray diffraction pattern obtained from the peeled surface. In the measurement, the conventional XRD equipment was used.

## 2. Experiments

### 2-1 Specimen preparation

Figure 4 shows the specimen preparation procedure. We thinned the specimen by polishing from both sides so that the interface layer between the wire and glass would maintain its original state, without being exposed to the air. In the thinning process, we observed the polished surfaces using an optical microscope to make sure that the thinning process was being conducted equally on both sides.

The aimed thickness after thinning was 200  $\mu\text{m}$ , which was sufficiently thin for the diffracted x-ray to penetrate. As we used a two dimensional (2-D) detector in the XRD measurements, the diffracting region should be approximated as a point. In this point of view, the aimed thickness was also appropriate.

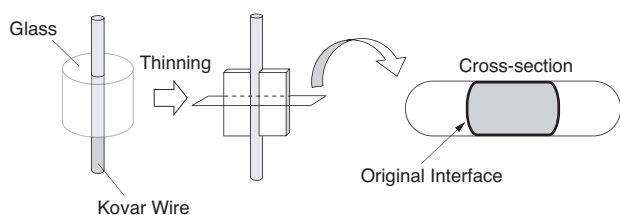


Fig. 4. Schematic figure of sample preparation

### 2-2 XRD measurements

As described thus far, the conventional XRD equipment could not give the x-ray with sufficient intensity and transmitted to analyze the extremely thin interface layer. Therefore, we utilized the highly brilliant x-ray in SPring-8, one of the largest synchrotron radiation (SR) facilities in the world. The measurements were carried out at BL16XU (SUNBEAM-ID). The x-ray energy was 25 keV and the

higher harmonics were cut by using an Rh-coated mirror placed at an incident angle of 1.5 mrad.

Here, we describe some of the important factors in the measurement in detail. The measurement configuration is illustrated in Fig. 5.

First of all, the incident x-ray beam was irradiated perpendicularly to the polished surface of the specimen (Fig. 5 (a)) and the diffracted x-ray was detected by the 2-D detector. The diffraction occurred not only in the interface layer but also on the polished surface of the Kovar wire, which should have been oxidized in the atmosphere. However, the diffraction from the polished surface could not penetrate the wire because of its large absorption coefficient for the x-ray. On the other hand, the diffraction from the interface layer could penetrate the glass, whose absorption coefficient was relatively small. Thus, we succeeded in detecting the diffraction from the aimed interface layer selectively.

Secondly, the shape of the incident x-ray beam was examined. Generally, as the beam size becomes larger, the undesired diffraction from the Kovar wire increases. Then we have to shorten the dwell time so that the 2-D detector would not be saturated. Therefore, we cannot obtain sufficient signals of the interface area. We adjusted the slits to make the x-ray beam width and height 5 mm and 20  $\mu\text{m}$ , respectively, in order to increase the signal from the aimed interface layer and to minimize the diffraction from other regions in the specimen. In controlling the beam shape, the parasitic scattering by the vertical slits was found to expand the beam size, which increased the background and lowered the sensitivity. To reduce the parasitic scattering, we placed two collimation slits in tandem geometry so that the vertical x-ray size to be 30  $\mu\text{m}$  extension was controlled small.

The third factor is the x-ray beam alignment. To maximize the diffraction from the aimed interface, the beam should be aligned to the interface as precisely as possible. Figure 6 shows the intensity of the transmitted x-ray that was measured by changing the position of the specimen. The position can be classified into four regions; air, glass,

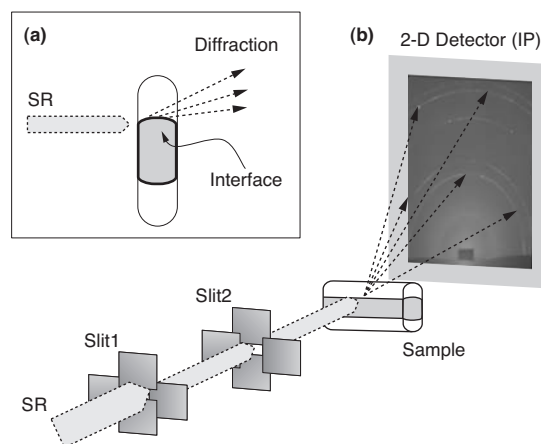


Fig. 5. X-ray diffraction measurement layout with synchrotron radiation (a) Cross section of sample (b) Layout of slit, sample and detector

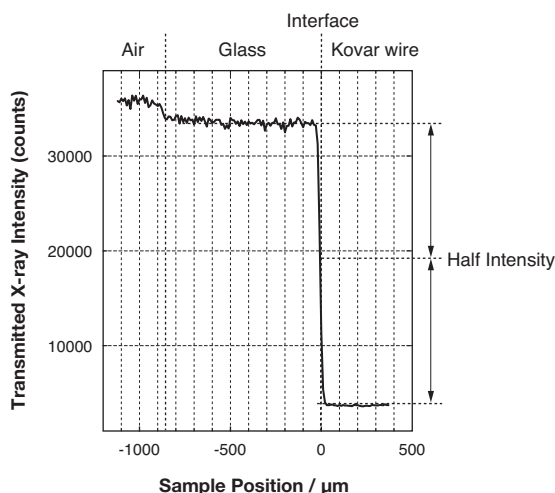


Fig. 6. Penetrating x-ray intensity vs. specimen position

interface, and Kovar wire. The point where the intensity became half of that of the glass region was defined as the interface. We found that the best position for the x-ray diffraction measurements was at 20  $\mu\text{m}$  from the interface toward the glass region.

Finally, we describe the effect of x-ray detectors. As the thickness of the interface layer is less than 1  $\mu\text{m}$ , there are not sufficient numbers of crystal grains to make a complete Debye ring. It follows that the conventional scanning of scintillation counter or 0-dimensional (0-D) detector would not work in the diffraction measurements. Therefore, we have utilized an imaging plate (IP, BAS-SR2040 released by FUJIFILM Corporation), which is a kind of 2-D detector.

Figure 7 shows an example of diffraction image obtained by the IP. The exposure time for the IP was limited to 5 minutes to avoid saturation in the diffraction peaks. The azimuth and camera length were corrected by measuring the reference of  $\text{CeO}_2$  powder. We found several incomplete Debye rings, which were assigned to Kovar. The bright spots on the rings indicate the poor uniformity of the Kovar crystal grain size in the narrow measurement domain of 500

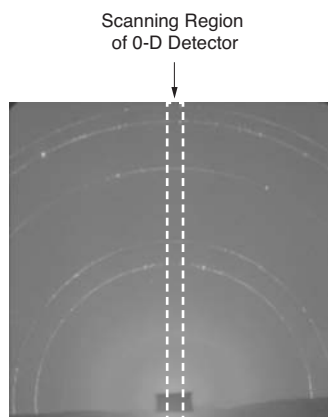


Fig. 7. X-ray diffraction pattern obtained with 2-D detector (IP)

$\mu\text{m} \times 30 \mu\text{m}$ . Needless to say, the number of the Fe oxide crystal grain should be much fewer than that of Kovar and it would be impossible to observe the Fe oxide diffraction peaks by using the 0-D detector scan, which gives only the limited region marked by the dashed line in Fig. 7. We integrated the 2-D diffraction image in the direction of circumference, using Fit2D code<sup>(2)-(7)</sup> released by European Synchrotron Radiation Facility (ESRF) in France, and obtained the spectra of diffraction intensity versus angle.

### 3. Result

Figure 8 shows the diffraction spectra of the interface layer and the glass region. Note that, in the horizontal axis, we have converted the diffraction angle into the case of using  $\text{Cu K}\alpha$  x-ray source (8.048 keV), which is widely used in commercially available XRD equipment. In both spectra, we see a broad peak around  $25^\circ$ , which is derived from the silicate glass. We also see sharp peaks at  $44^\circ$  and  $51^\circ$ , which correspond to those of Kovar. The Kovar peaks have been found as well in the Fig. 8 (b) (glass region), though their relative intensities compared to the broad peak are much smaller than those in Fig. 8 (a). The tail of the incident x-ray beam is considered to be irradiating in the Kovar area, though the beam center is aiming at the glass region.

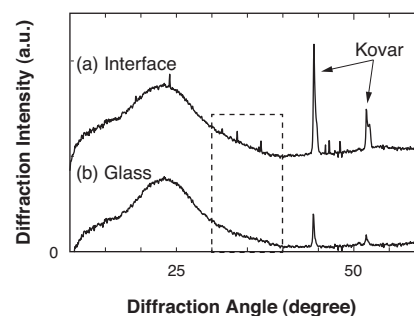


Fig. 8. X-ray diffraction patterns of thinned sample (wide range)

Figure 9 shows the enlargement of the area surrounded by dashed line in Fig. 8. The Fe oxides are known to have diffraction peaks in this angle range. We have confirmed the peaks of  $\text{Fe}_2\text{O}_3$  and  $\text{FeO}$  in the spectrum of the interface layer. On the other hand, no such peaks were found in the glass region. These results demonstrate that the Fe oxides exist at the metal/glass interface. In the measurements using the peeling-off specimens and commercially available XRD equipment, we could not observe the oxide peaks. The techniques that we have developed for the specimen fabrication and diffraction measurement are very useful to observe the thin interface layer.

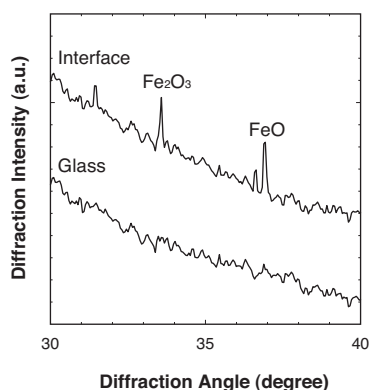


Fig. 9. Magnified x-ray diffraction patterns of thinned sample at iron-oxide region

#### 4. Conclusion

We have successfully developed the new technique to analyze the interface between metal and glass nondestructively. In the specimen fabrication, we employed the precise polishing technique instead of the conventional exfoliating, so that the interface could maintain its original state. In the diffraction measurements, we combined the highly brilliant x-ray from synchrotron radiation and 2-D detector. We also optimized the specimen configuration, x-ray beam shape, and its alignment. As a result, we succeeded in detecting the diffraction peaks from the extremely small quantity of Fe oxides that existed in the 1  $\mu\text{m}$  thick metal/glass interface.

The analyses technique developed in this study is very useful to investigate the bonding mechanism between heterogeneous materials. We will apply this technique to other materials and develop new products with superior adhesiveness in the future.

#### 5. Acknowledgements

The synchrotron radiation experiments were performed at the BL16XU of SPring-8 with the approval of the Japan Synchrotron Radiation Research Institute (JASRI) (Proposal No. 2009A5031).

· Kovar is a trademark or registered trademark of CRS Holding, INC. in the U.S. and other countries.

#### References

- (1) Y. Ikeda and K. Samejima, *J. Soc. Mater. Sci.*, 10 (1961) 792.
- (2) A P Hammersley, ESRF Internal Report, ESRF97HA02T, (1997)
- (3) A P Hammersley, ESRF Internal Report, ESRF98HA01T, (1998)
- (4) A P Hammersley, S O Svensson, and A Thompson, *Nucl. Instr. Meth.*, A346, 312-321, (1994)
- (5) A P Hammersley, S O Svensson, and A Thompson, H Graafsma, Å Kvik, and J P Moy, *Rev. Sci. Instr.*, (SRI-94), 66, 2729-2733 (1995)
- (6) A P Hammersley, K Brown, W Burmeister, L Claustre, A Gonzalez, S McSweeney, E Mitchell, J-P Moy, S O Svensson, A Thompson, *J. Syn. Rad.*, 4, 67-77, (1997)
- (7) A P Hammersley, S O Svensson, M Hanfland, A N Fitch, and D Häusermann, *High Pressure Research*, 14, pp235-248, (1996)

#### Contributors (The lead author is indicated by an asterisk (\*).)

##### J. IIHARA\*

- Doctor of Science,  
Senior Assistant General Manager, Analysis  
Technology Research Center, R&D Laboratories



##### K. YAMAGUCHI

- Doctor of Engineering,  
Senior Assistant General Manager, Analysis  
Technology Research Center, R&D Laboratories

